Spontaneous Initiation and Termination of Complex Rhythms in Cardiac Cell Culture

GIL BUB, PH.D., KATSUMI TATENO, PH.D., ALVIN SHRIER, PH.D., and LEON GLASS, PH.D.

From the Department of Physiology, McGill University, Montreal, Quebec, Canada

Complex Cardiac Rhythms. ***Introduction:*** **Complex cardiac arrhythmias often start and stop spontaneously. These poorly understood behaviors frequently are associated with pathologic modification of the structural heterogeneity and functional connectivity of the myocardium. To evaluate underlying mechanisms, we modify heterogeneity by varying the confluence of embryonic chick monolayer cultures that display complex bursting behaviors. A simple mathematical model was developed that reproduces the experimental behaviors and reveals possible generic mechanisms for bursting dynamics in heterogeneous excitable systems.**

Methods and Results: **Wave propagation was mapped in embryonic chick myocytes monolayers using calcium-sensitive dyes. Monolayer confluence was varied by plating cultures with different cell densities and by varying times in culture. At high plating densities, waves propagate without breaks, whereas monolayers plated at low densities display spirals with frequent breaks and irregular activation fronts. Monolayers at intermediate densities display bursting rhythms in which there is paroxysmal starting and stopping of spiral waves of activity. Similar spatiotemporal patterns of activity were also observed as a function of the time in culture; irregular activity dominates the first 30 hours, followed by repetitive bursting dynamics until 54 hours, after which periodic target patterns or stable spirals prevail. In some quiescent cultures derived from older embryos, it was possible to trigger pacemaker activity following a single activation. We are able to reproduce all of these behaviors by introducing spatial heterogeneity and varying neighborhood size, equivalent to cell connectivity, in a spontaneous cellular automaton model containing a rate-dependent fatigue term.**

Conclusion: **We observe transitions from irregular propagating waves, to spiral waves that spontaneously start and stop, to target waves originating from localized pacemakers in cell culture and a simple theoretical model of heterogeneous excitable media. The results show how physiologic properties of spontaneous activity, heterogeneity, and fatigue can give rise to a wide range of different complex dynamic behaviors similar to clinically observed cardiac arrhythmias.** *(J Cardiovasc Electrophysiol, Vol. 14, pp. S229-S236, October 2003, Suppl.)*

paroxysmal tachycardia, optical mapping, heterogeneity, cell coupling, reentry, mathematical models

Introduction

Although some cardiac arrhythmias are sustained in the absence of a therapeutic intervention, in most cases cardiac arrhythmias start and stop spontaneously. The intervals between bouts of tachycardia can be quite variable, and the determinants of the intervals are poorly understood. In a small percentage of patients, there are repetitive or incessant bursts of paroxysmal tachycardia imposing a virtually continuous arrhythmia.[1,2]

Paroxysmal tachycardia is characterized by an unpredictable mixture of sinus rhythm and runs of tachycardia of variable duration. The unpredictability of these arrhythmias may be caused by a complex interaction of spontaneous cells and the underlying substrate. The origins of paroxysmal tachycardias are not well understood, but it appears that, in some cases, they can be driven by extrasystolic events that trigger runs of reentrant activity.[3] The nature of the activation patterns is difficult to predict because pacemakers can intermittently propagate waves, which may fragment to generate reentrant circuits in a manner that sensitively depends on local coupling as well as the geometry and heterogeneity of the substrate.[4] Recent studies have underscored the importance of local variations in the geometric arrangements of cells, especially under conditions of poor cell-cell coupling.[5] Variations in geometry may act to block or enhance propagation[6] and may result in a preferred direction of propagation,[7] whereas coupling strength may act to suppress propagation from pacemaking sites.[8] Although it also is unclear why paroxysmal tachycardia spontaneously stops, it previously was shown that rate-dependent changes in excitability can contribute to complex rhythms in tissue culture studies.[9]

Paroxysmal reentrant wave activity has been found in spontaneously beating embryonic chick heart cell monolayer cultures.[9] In this study, we exploit this system to evaluate the effects of monolayer confluence on the dynamics of wave propagation. We observe an organization of the patterns of wave dynamics determined by the degree of substrate heterogeneity and cell interaction. This behavior can be simulated using a simple mathematical model of a heterogeneous network with spontaneously excitable cells and a rate-dependent fatigue term. From these results, we propose a global

Supported by the Canadian Institutes for Health Research, the Canadian Heart and Stroke Foundation, MITACS, and the NIH Research Resource for Complex Physiologic Signals.

Address for correspondence: Leon Glass, Ph.D., Department of Physiology, McGill University, 3655 Drummond Street, Montreal, QC, Canada H3G 1Y6. Fax: 514-398-7452; E-mail: glass@cnd.mcgill.ca

doi: 10.1046/j.1540.8167.90315.x

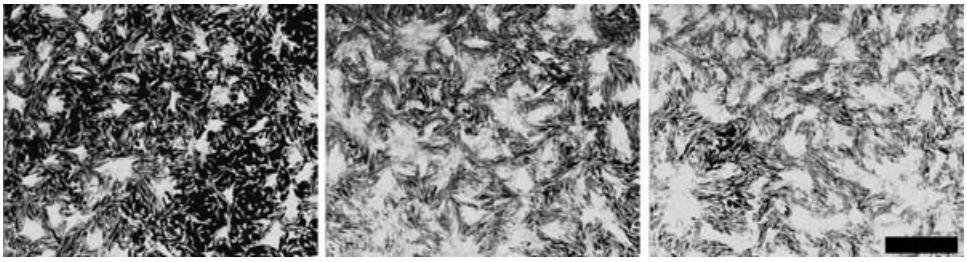

Figure 1. *High-resolution images of the cardiac monolayer preparation plated at different densities at 72 hours in culture. Left panel: Low density (5 × 10^3 cells/mm^2). Middle panel: Intermediate density (10 × 10^3 cells/mm^2). Right panel: High density (20 × 10^3 cells/mm^2). The scale bar is 500 μm. Each panel images a 2.4 × 2.4-mm area near the center of an 8-mm-diameter monolayer.*

organization of paroxysmal dynamics as a function of tissue heterogeneity in excitable systems.

Methods

Culture

In brief, as described previously,[9] chick embryonic ventricular heart cells were enzymatically isolated and plated on lysine-coated dishes for 30 to 72 hours in maintenance medium 818a at 36°C. In the present study, cells were plated at varying densities (5 to 20 × 10^3 cells/cm^2) and were loaded with either Calcein-AM (5 μM, 45 min) to monitor confluence or calcium green (5 μM, 30 min) to monitor intracellular calcium dynamics. Alternatively, the cells were fixed and stained with a Masson trichrome stain to determine the fraction of fibroblasts in culture; at 72 hours, the monolayer consists of up to 10% fibroblasts. Seven-day-old embryos were used for the experiments on spiral wave bursts and targets (Figs. 1–3). We used 10-day-old embryos when investigating triggered activity in order to lower the number of spontaneous pacemakers in culture.[10]

Imaging

The optical mapping experiments were conducted as described previously.[9] In brief, a macroscope was used to perform low-light-level measurements at low magnification scales (objective: Nikon 80 mm, imaging lens Chromicar Zoom 130, excitation filter 460 nm, dichroic beam splitter at 510, imaging filter 540, Omega optical). The macroscope was mounted over an inverted microscope (Zeiss Axiovert 125M) to allow for simultaneous monitoring of the monolayer dynamics at macroscopic and microscopic scales. Images were collected using a cooled CCD camera (model TE CCD 576, Princeton Instruments) at 20 frames per second. Adjacent pixels in the CCD were binned (2 × 2) and up to 30,000 consecutive images were transferred directly to a computer for storage and analysis. Image data from each binned pixel was scaled based on its maximal range over 20 frames, and the image was spatially averaged, background subtracted, and viewed using custom-written software. Calcium-sensitive dyes were used to allow long recording times with high signal-to-noise ratios while minimizing phototoxic damage. Waves mapped with calcium-sensitive dyes follow the same patterns as waves mapped with voltage-sensitive dye. Movies of waves

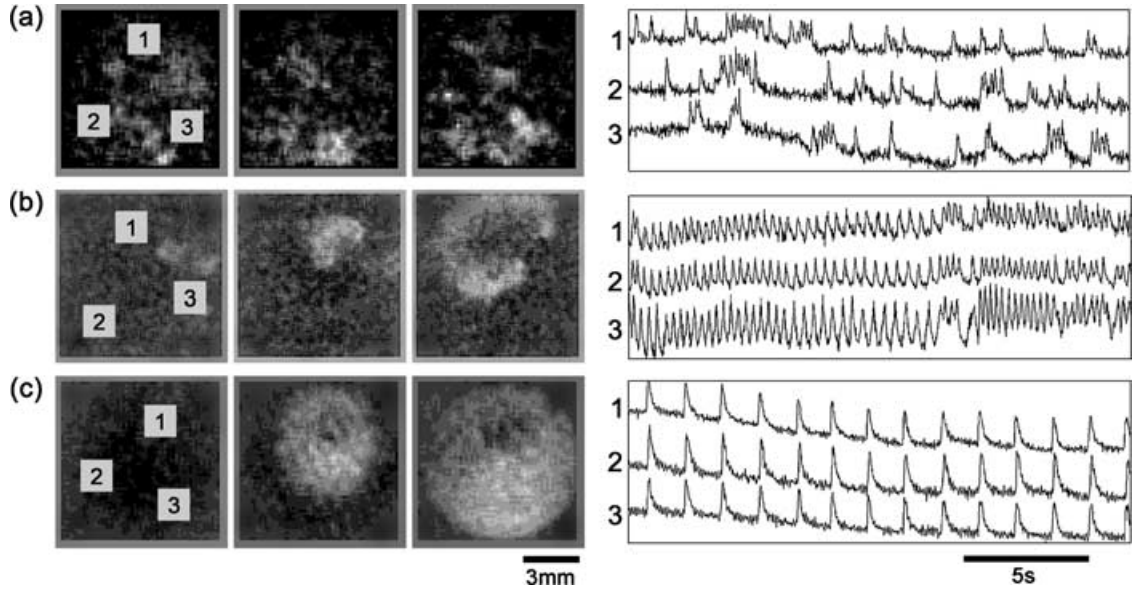

Figure 2. *Calcium fluorescence recorded from monolayers with different plating densities after 3 days in culture. Each image is separated by 150 msec. The rightmost panel in each row shows fluorescence plotted against time for 20 seconds of recorded data for the three subregions shown in the first panel of each row. a: Low density—irregular fractured activity. b: Intermediate density—spiral wave propagation. c: High density—target patterns.*

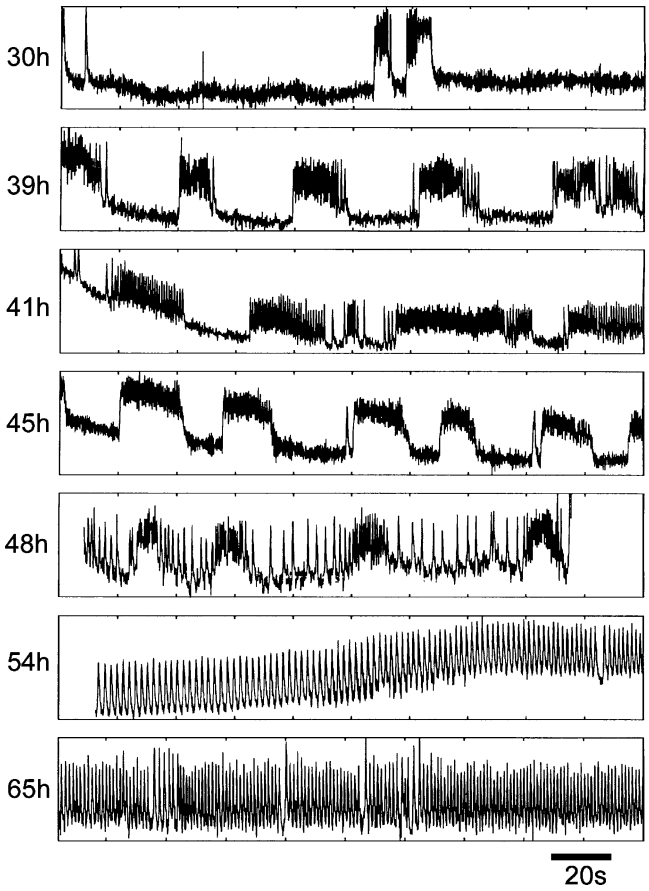

Figure 3. *Calcium fluorescence recorded from monolayers plated at intermediate densities (10×10^3 cells/mm^2) as a function of culture age. At 30 hours, behavior is disorganized, with occasional bursts of activity. At 39 to 45 hours, regular bursts of activity are observed. These bursts are generated from the spontaneous onset and offset of spiral waves. At 48 hours, spiral bursts and target patterns are seen. At 54 hours, stable spirals are observed. At 65 hours, target patterns are observed. Each trace was recorded for 200 seconds. Traces were obtained by averaging a 4 × 4 pixel area at the center of the imaging frame.*

measured with calcium- and voltage-sensitive dyes are available online at *www.cnd.mcgill.ca/bios/bub/movies.html*.

Mathematical Modeling

In order to capture the main qualitative features of the dynamics, we adapt cellular automata model based on an earlier model originally proposed by Greenberg and Hastings.[11] The choice of cellular automaton model over an ionic model is based on the following considerations. First, the dynamics observed in the culture system strongly depends on random heterogeneities that cause conduction block. In order to investigate the effects of randomly distributed heterogeneities, we need to simulate many randomly generated geometries, which is not practical in more computationally intensive ionic models. Second, we measure macroscopic wave patterns in this study and do not measure ionic currents. Therefore, we believe that we do not have adequate information to generate a defendable ionic model. Third, because the cellular automaton model is a general model of excitable media, the results should apply to a wide range of cardiac systems and should be reproducible in appropriately designed ionic models.

The cellular automaton is formulated as follows. Each site at time (t) is assigned a state, $u_i(t)$, where the subscript refers to the cell number. The state is an integer: 0 is a rest state; states $1, 2, \ldots, E$ are excited states; states $E+1$, $E+2, \ldots, E+R$ are refractory states; state $(E+R+1)$ is identified with the rest state 0. The update rule for the state of a site is as follows: if $1 < u_i(t) < (E+R)$, then $u_i(t+1) = u_i(t) + 1$. If $u_i(t) = 0$, then $u_i(t+1) = 0$, unless u_i is excited by its neighbors, or it is spontaneously excited. A fixed number (5%) of the points in the grid are pacemakers. Each pacemaker spontaneously fires with a fixed period T, but the periods of the different pacemakers are assumed to be different. If a pacemaker is activated by a propagating wave, then its pacemaker cycle will be reset.

We introduce spatial heterogeneity in the cell density by perturbing the location of each cell. We take the nearest neighbor distance between cells to be 1.[12] Given the original coordinates (x_0, y_0), the new coordinates are $(x_0 + ex, y_0 + ey)$, where *ex, ey* are uniformly distributed in the interval $(-0.5, 0.5)$. The condition for an unexcited cell i to become excited is as follows. If $u_i(t) = 0$, then $u_i(t+1) = 1$ if:

$$\frac{\sum_{D[j,i]<r;0<u_j(t)\leq E} S_j}{\sum_{D[j,i]<r;u_j(t)=0 \text{ or } u_j(t)>E} S_j} > \theta, \qquad (1)$$

where $D[j, i] = |x_j - x_i| + |y_j - y_i|$ is the distance between cell j and cell i, (x_j, y_j) is the location of cell j, θ is the excitation threshold, and the summation is over all cells within a distance r of cell i. We call r the neighborhood size. In this formulation, an older or denser culture is represented by a larger value of r. Excitation is determined by the ratio of excited to nonexcited cells in the neighborhood of a given cell. We introduce a fatigue term γ,where $\gamma_i(t+1) = \gamma_i(t) + F_{add}$ if $u_i(t+1) = 1$, and $\gamma_i(t+1) = (\gamma_i(t) \times F_{sub})$ if $u_i(t+1) \neq 1$. The fatigue term is added to a minimum threshold value $\theta_{min,}$ and the threshold is set to $\theta = \theta_{min} + \gamma(t)$. As a consequence of the fatigue, the propagation velocity slows and there is a greater tendency to have excitation blocked following periods of rapid activity. The parameters used in all simulations are $\theta = 0.30$, $E = 12$, $R = 13$, $F_{add} = 0.02$, and $F_{sub} = 0.999$, with variable neighborhood size r. The number of pacemaker cells is 5% of the total, and each is assigned a period randomly chosen between 180 and 220 time steps.

Results

Bursting Reentrant Rhythms

The effect of monolayer confluence on calcium wave dynamics was determined by plating ventricular cells derived from 7-day-old embryonic chicks at three different densities. Figure 1 illustrates the changes in appearance as cell density increases. Low-density monolayers are characterized by large gaps and irregular cell spacing. As density increases, the size of the gaps decrease and the monolayers appear less heterogeneous. Figure 1, left panel, shows a monolayer plated at a low density (5×10^3 cells/cm^2). Gaps can be as large as 500 μm in diameter. At an intermediate density (10×10^3 cells/cm^2), gaps are less apparent and usually are smaller than 30 μm in diameter (Fig. 1, middle panel). At high plating densities (20×10^3 cells/cm^2), the monolayer has very few detectable gaps or holes (Fig. 1, right panel). The percent area covered by cells was determined by loading the monolayer with

Calcein. All cells in the preparation were brightly stained with this dye, thus allowing empty spaces to be easily seen. All pixels above a fixed luminosity (75% of the maximum value) were counted, and the total was divided by the number of pixels in each image. The density was determined from 5 images (2 near the edge, 3 near the center) obtained from three monolayers at each density. Low-density monolayers cover 54% ± 4% of the total area, intermediate-density monolayers cover 73% ± 9 of the total area, and high-density monolayers cover 92% ± 6 of the total area.

Figure 2 shows fluorescent images captured at 150-msec intervals at each plating density. The rightmost panel for each series illustrates the summed fluorescence activity within a rectangular area at three sites on the monolayer for a period of 20 seconds. The rectangular areas are shown in the first panel of each series. The time traces indicate how the activities at different areas of the preparation are correlated in time. For low plating densities, waves are fractured and form spirals with irregularly shaped activation fronts (Fig. 2a). Activation fronts frequently break and form new spiral centers. Wave speed is 12 ± 2 mm/s (n = 6) for planar wavefronts but is lower and highly variable for curved and meandering wavefronts. The time traces demonstrate that the activity is irregular as the traces are not always correlated. For intermediate plating densities, we observe spiral waves with a small number of spiral centers (Fig. 2b). Wavefronts appear to be smooth and display wavebreaks far less frequently than low-density preparations. The time traces for this record are rapid but synchronous. These spirals are either stable or display a bursting rhythm. Wave speeds are 24 ± 3 mm/s (n = 6) for wavefronts far from spiral cores and are slower and more variable near spiral cores. At high plating densities, monolayers display target patterns or stable spiral waves with no wavebreaks (Fig. 2c). Wave speeds for high-density monolayers are 33 ± 2 mm/s (n = 6) for wavefronts with low curvature.

The effect of incubation time in culture on the dynamics of the monolayers was systematically explored. The calcium fluorescence from six monolayers plated at identical densities from the same culture with varying incubation times is shown in Figure 3. Infrequent bursts of activity appeared after 24 hours in culture. The frequency and duration of the bursts subsequently increased over the next 24 hours. By 54 hours, activity became regular, with infrequent short breaks. At 68 hours, the dynamics are periodic. Spirals were clearly observed at every time point except the one measured at 68 hours. In this case, the periodic rhythm was generated by a regularly beating focus. At 54 hours, the regular beating was generated by a stable spiral. Similar behavior was observed in three experiments.

Triggered Bursting Rhythms

The bursting dynamics described earlier are associated with reentrant activity. However, in 6 of 30 cultures plated for 72 hours derived from 10-day-old embryonic chick hearts, bursts of activity were associated with target patterns of excitation. As shown in Figure 4, a wave of excitation is spontaneously triggered from the region indicated in black, but the subsequent beats originate from a new source shown in gray. This triggered burst persists for 93 seconds before activity spontaneously terminates. Following a pause of about 36 seconds, there is a second spontaneous initiation. The first beat of the second burst initiates at a different location, but the subsequent beats all seem to be initiated from the same triggered locus.

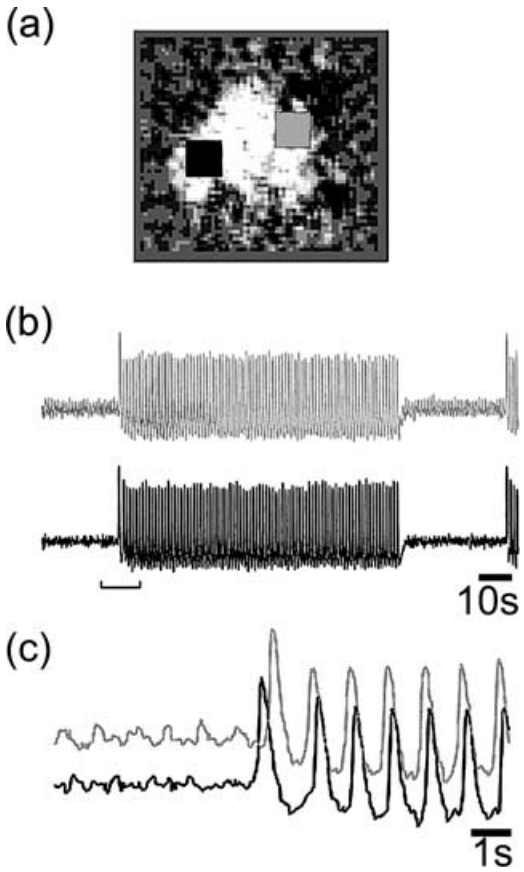

Figure 4. *Triggered activity. a: Calcium fluorescence from a monolayer of embryonic heart cells cultured after 10 days. b: Fluorescence from the two regions shown in panel a. The spontaneous activity originating near the black square on the first beat triggers activity from the neighborhood of the gray square. Waves propagate as target patterns from both foci. c: Enlargement of the initiation of the first burst of activity shown in trace b.*

Mathematical Modeling

The experimental results display an organization of dynamics that depend upon monolayer confluence and heterogeneity. To help understand the origins of the observed dynamics, we developed a simple cellular automaton model that accounts for variations in geometry by simulating the effect of current sources and sinks.[4,13] Spontaneous activity is added by having a small fraction of the cells beat with a fixed period randomly chosen within an interval. Previous studies by our group[14] and others[15] have shown that excitation can be reduced by prolonged runs of rapid activity. A rate-dependent decrease in excitability is added by introducing a fatigue term that increases the excitation threshold as a function of activity. The model is used to determine general modes of behavior as a function of excitability and coupling without taking into account specific ionic properties of the cells.

Figure 5 shows the dynamics of the model for three different neighborhood sizes, which serves to simulate variation in confluence as reflected by changes in the extent of cellular connectivity. For neighborhood size, $r = 1.25$, the model displays irregular activity (Fig. 5a). The patterns of

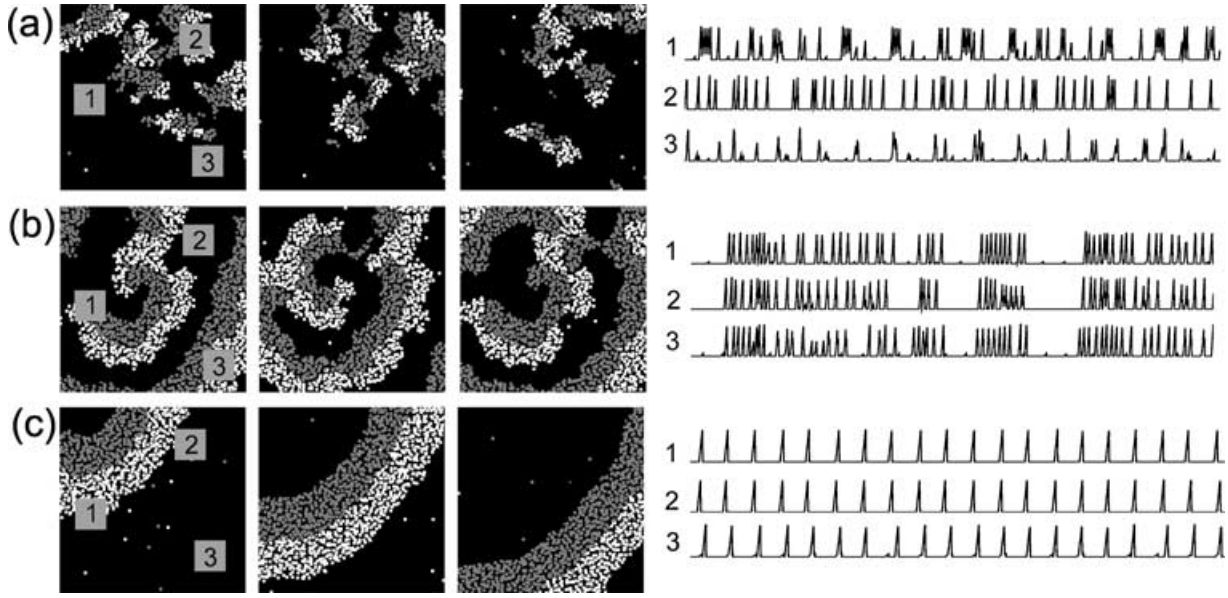

Figure 5. *Dynamics associated with the model for three different values of r. In each row, the panels show snapshots of the activity in 20 iterate intervals, and the traces show the activity over 4,000 iterates sampled from cells within the square regions in the first panel of the series. A cell $u_i(t)$ is colored according to the following: if $(0 < u_i(t) < E)$ (active) it is colored white; if $(E < u_i(t) < R)$ (refractory) it is colored gray; and if $u_i(t) = 0$ (refractory) it is colored black. a: $r = 1.25$; b: $r = 1.5$; c: $r = 1.75$.*

activation are not synchronous for different regions of the grid. The model displays bursting dynamics with its neighborhood set to $r = 1.5$. Unidirectional block at the initiation site generates spiral waves. The spiral tip tends to increase its meander as fatigue accumulates. The spiral tip eventually collides with the boundary of the domain, terminating activity. This process repeats, giving rise to a bursting rhythm (Fig. 5b). For $r = 1.75$, the model displays target patterns. Spirals do not form because broken wavefronts seal at the initiation site, and the wave does not develop wavebreaks as it travels across the array.

The model also can display triggered activity for large neighborhood sizes, which would reflect a high degree of cell connectivity. As neighborhood size increases, initiation of spirals and targets decreases. Triggering in the model occurs when a wave acts to synchronize the pacemakers, which increases the likelihood of subsequent activations. Pacemakers become desynchronized over time, because faster pacemakers fire before the majority and are refractory to phase resetting. This behavior is shown in Figure 6 for $r = 2.15$. A plane wave is initiated at the top of the grid. The next beat comes from a spontaneously initiated target wave coming from the left edge of the grid. The target beats seven times and then stops.

The dynamics are strongly dependent on the underlying geometry of the grid. For example, the same parameter values can give rise to stable target waves and bursting spirals for two different arrays. We quantify the behavior of the model by running simulations for 100 different randomly assembled grids over a range of neighborhood sizes. The number of arrays that generate a spiral within 10,000 iterates is shown by the bars with dashed lines in Figure 7. The probability of generating a spiral wave is highest at $r = 1.65$ and falls off rapidly as r increases. Triggered activity is tested by initiating a plane wave at the top of the array after the 10,000th iterate. The array is scored as generating triggered activity if the array was quiescent (no targets or spirals were detected 2,000 iterates prior to the plane wave), and a target wave is initiated within 400 iterates of the plane wave. The probability of observing triggered activity is highest at $r = 2.1$ and falls off gradually as r increases.

Discussion

In this study, we observed a transition from blocked propagation, to fractionated spiral waves, to bursting spirals, to periodic target waves of activity as a function of monolayer culture confluence. We also propose a very simple mathematical model of a randomly assembled network of spontaneously active cells that demonstrates these same

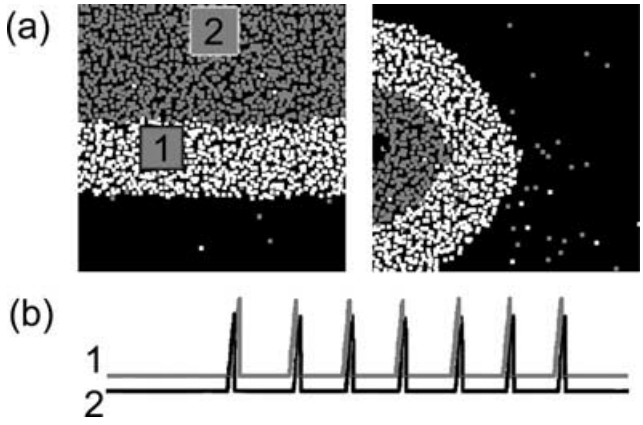

Figure 6. *Triggered activity in the simulation for $r = 2.15$. a: A planar wave is initiated at the top of the grid. It triggers a group of pacemakers at the left of the grid. b: The activity over 2,000 iterates for the cells shown in the numbered boxes in the first panel. At first, the wave triggers the cells in box 2 then in box 1, but subsequent beats are initiated near box 1.*

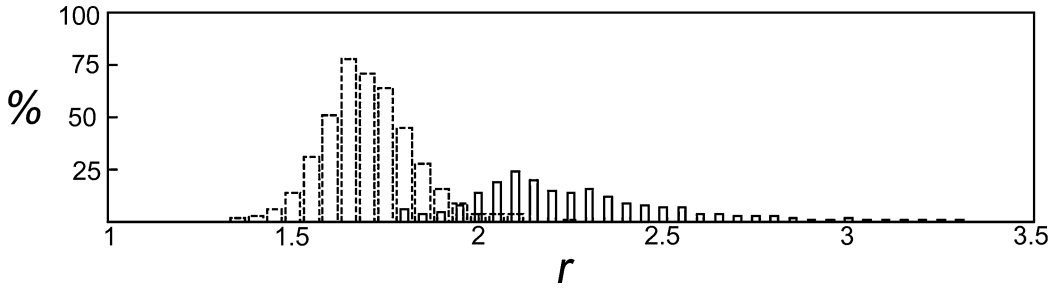

Figure 7. *Fraction of geometries generating spiral waves and triggered activity as a function of neighborhood size. The fraction was determined by running the model for 100 different arrays for each parameter value. Histograms from simulation runs that resulted in the spontaneous generation of a spiral wave within 10,000 iterates are plotted with dashed lines. Histograms from simulations in which the array is quiescent for 2,000 iterates, and a plane wave impulse triggers a target wave within 400 iterates, are plotted with solid line bars.*

behaviors as neighborhood size is varied. We propose that the behaviors observed in the experimental system and in the mathematical model capture important spatiotemporal patterns of activity that, in general, may be expected in heterogeneous excitable media such as the heart, as the parameters describing the spontaneous activity, coupling, and fatigue are varied. In particular, the dynamics observed here could apply to a variety of disease conditions that evoke paroxysmal bursts of cardiac tachycardia, particularly due to localized disruption of the anatomic and/or physiologic substrates.

In the current study, we chose to use monolayer cultures because their heterogeneity can be experimentally manipulated and complex dynamics can be imaged using fluorescent dyes. Long-duration recordings with high spatial resolution are necessary to elucidate the spatiotemporal patterns seen in our preparation. We optimized our recording system to be able to follow the evolving patterns of wave dynamics with high spatial resolution over 30 minutes. To achieve this end, we chose calcium-sensitive dyes because they have a high signal-to-noise ratio and have low phototoxic effects.[4,8,9] Calcium fluorescence closely follows the signal generated by voltage-sensitive dyes[16] and thereby reflects the pattern of cardiac monolayer excitation. We previously used this approach to demonstrate reentry in sheets[4,9] and cultured rings.[17] More recently, a similar approach was used by others to investigate a cell culture model of reperfusion injury.[8] High-temporal, low-spatial-resolution studies of conduction have been carried out by other groups using voltage-sensitive dyes[6,7,18] and extracellular electrode arrays.[19]

Over the past decade, we have studied a number of different experimental preparations in which there are paroxysmal repetitive bursts of activity, and we also developed mathematical models of the observed dynamics.[9,14,17,20] A prototypical example of a bursting rhythm was generated by stimulating a spontaneous pacemaker at a fixed delay after detection of the action potential.[14] In this model, the rapid activity caused a fatigue effect that eventually blocks activity. Following termination of the stimulation, the intrinsic cycle length gradually returned to its control value as the fatigue term dissipated. We propose that similar mechanisms are present in other experimental models of tachycardia. An experimental model of an accessory pathway can be developed by stimulating the atria at a fixed delay following ventricular activation.[21-23] For appropriate values of delay time, there are paroxysmal bursts of reentrant rhythm. Similar types of rhythms may be established in tissue culture. When cardiac cells were cultured in a ring-shaped geometry, we observed a variety of rhythms, including waves emanating from a pacemaker that propagated around the ring in both directions and collided and annihilated at the antipodal point, circulating reentrant waves, and reentrant waves that spontaneously initiated and terminated.[17] We have hypothesized that the spontaneous initiation of the reentrant waves occurred as a consequence of spontaneous firing of a pacemaker coupled with unidirectional block due to heterogeneities in the preparation. Based on the observations in the preparations described earlier, we hypothesize that the more rapid activation associated with the reentry leads to a decrease in the excitability of the preparation and subsequent block of activity.

We hypothesize that the initiation of the spiral waves in our monolayer cultures occurs as a consequence of localized spontaneous activity followed by unidirectional block.[9] We believe that unidirectional block occurs in these preparations because the cells are sparse and not very well coupled so that the heterogeneities can lead to locally blocked propagation and broken waves, thus setting the conditions for reentry. This hypothesis is supported by the experimental results demonstrating that the bursting dynamics only occurs over a limited range of densities and developmental ages. Once the reentrant wave is established, it executes several rotations but eventually terminates. In similar fashion to the behavior described earlier, we believe that the termination is associated with a reduction of excitability consequent to the rapid activity. This mechanism is captured in the theoretical model.

The monolayer preparation also displays triggered activity. Triggered activity usually is attributed to oscillations in membrane potential, called afterdepolarizations,[24] caused by ionic events at the cell level.[25] In some cases, this is attributed to calcium overload leading to a secondary increase in sodium conductance.[26,27] Triggered activity occurs soon after or during the triggering pulse, and more than one pulse generally is required to initiate the arrhythmia. In addition, the arrhythmia is associated with afterdepolarizations typically faster than the intrinsic rate. In the present study, we found that a single pulse is sufficient to trigger the spontaneous activity, and the spontaneous activity is initiated with a relatively long delay after the stimulus. This behavior is similar to pause-induced early afterdepolarizations seen in long QT arrhythmias[28,29]; however, the period of triggered activity in the monolayers is too long to be accounted for by this mechanism. Consequently, we do not consider

afterdepolarizations to be the likely cause of the triggered response. Coupling strength previously has been shown to modulate the activity of pacemakers and excitable cells.[8] Mathematical models of a single pacemaker cell coupled to an excitable cell display complex dynamics that may explain intermittent activity from ectopic foci.[30] We also observe coupling-dependent propagation in the cellular automaton model and propose a mechanism based on oscillator synchrony. The cellular automaton displays a decrease in automaticity as coupling is increased. This occurs because a larger number of cells must be simultaneously active in order to propagate a wavefront. A pulse acts to synchronize oscillators, leading to propagation of one or more target waves. The observed dynamics strongly depends on the local geometry. We observe triggering in approximately one fourth of randomly generated arrays for some neighborhood sizes.

Earlier cellular automaton models showed that heterogeneity in cell spacing generates wavebreaks for small neighborhood sizes but allows smooth propagation with large neighborhood sizes.[4] Varying the neighborhood size r changes the effective diffusion coefficient of the model[13] and simulates changes in cell-cell coupling and connectivity in the cell culture system. Further, we represent in a simple way the observation that rapid activity often can lead to "fatigue" characterized by reduced excitability. Clearly, the current model is not meant to substitute for ionic models of cardiac activity. However, by making clear key features that may account for complex behavior, we indicate directions for future research. We suggest that once more realistic models incorporate spontaneous activity, heterogeneity, and fatigue, it should be possible to generate rhythms of comparable complexity to what has been observed in this simple model. This will be particularly important for modeling complex arrhythmia, because the anatomic and physiologic substrates for diseased hearts often show significant deviations from normal hearts, including often modified geometry and heterogeneity subsequent to the disease process.

A wide variety of arrhythmias display paroxysmal bursts of activity. Examples include AV reciprocating tachycardia in patients with Wolff-Parkinson-White syndrome, repetitive monomorphic tachycardia,[31] ectopic atrial tachycardia, AV nodal tachycardia, and atrial fibrillation.[32,33] Although in some instances the anatomic and physiologic substrates of these rhythms are reasonably well understood and there are adequate means of treatment, in other situations the anatomic and physiologic bases of the tachycardias are not understood.[34] Further, despite the significant gains that have been made in theoretical modeling of reentrant arrhythmias in a variety of anatomies, the sorts of subtle dynamics that we have been studying here are not yet well understood or appreciated. We hypothesize that the same factors that underlie the starting and stopping of tachycardias in our model systems contribute to the generation of complex arrhythmia in the diseased myocardium.

References

1. Parkinson J, Papp C: Repetitive paroxysmal tachycardia. Br Heart J 1947;9:241-262.
2. Krikler D, Curry P, Attuel P, Coumel P: "Incessant" tachycardias in Wolff-Parkinson-White syndrome. I: Initiation without antecedent extrasystoles or PR lengthening, with reference to reciprocation after shortening of cycle length. Br Heart J 1976;38:885-896.
3. Taylor AD, Gross JG, Thorn SL, Lewis CT, Marshal AJ: New insights into onset mechanisms of atrial fibrillation and flutter after coronary artery bypass graft surgery. Heart 2002;88:499-504.
4. Bub G, Shrier A, Glass L: Spiral wave generation in heterogeneous excitable media. Phys Rev Lett 2002;88:058101-1-058101-4.
5. Spach MS, Heidlage JF: The stochastic nature of cardiac propagation due to the discrete cellular structure of the myocardium. Circ Res 1995;76:366-380.
6. Rohr S, Kleber A G, Kucera J: Optical recording of impulse propagation in designer cultures: Cardiac tissue architectures inducing ultra-slow conduction. Trends Cardiovasc Med 1999;9:173-179.
7. Rohr S, Kucera JP, Fast VG, Kleber AG: Paradoxical improvement of impulse conduction in cardiac tissue by partial cellular uncoupling. Science 1997;275:841-844.
8. Arutunyan A, Swift L, Sarvazyan N: Initiation and propagation of ectopic waves: insights from an in vitro model of ischemia-reperfusion injury. Am J Physiol Heart Circ Physiol 2002;283:H741-H749.
9. Bub G, Glass L, Publicover NG, Shrier A: Bursting calcium rotors in cultured cardiac myocytes monolayers. Proc Natl Acad Sci USA 1998;95:10283-10287.
10. Clay JR, Shrier A: Developmental changes in subthreshold pace-maker currents in chick embryonic heart cells. J Physiol 1981;312:491-504.
11. Greenberg JM, Hastings SP: Spatial patterns in discrete models of diffusion in excitable media. SIAM J Appl Math 1978;34:515-523.
12. Markus M, Hess B: Isotropic cellular automaton for modeling excitable media. Nature 1990;347:56-58.
13. Bub G, Shrier A: Propagation through heterogeneous substrates in simple excitable media models. Chaos 2002;12:747-753.
14. Kunysz AM, Shrier A, Glass L: Bursting behavior during fixed-delay stimulation of spontaneously beating chick heart cell aggregates. Am J Physiol 1997;273:C331-C346.
15. Gilmour RF, Salata JJ, Zipes DP: Rate-related suppression and facilitation of conduction in isolated canine cardiac Purkinje fibers. Circ Res 1985;57:35-45.
16. Fast VG, Ideker RE: Simultaneous optical mapping of transmembrane potential and intracellular calcium in myocytes cultures. J Cardiovasc Electrophysiol 2000;11:547-556.
17. Nagai Y, Gonzalez H, Shrier A, Glass L: Paroxysmal starting and stopping of circulating waves in excitable media. Phys Rev Lett 2000;84:4248-4251.
18. Entcheva E, Lu SN, Troppman RH, Sharma V, Tung L: Contact fluorescence imaging of reentry in monolayers of cultured neonatal rat ventricular myocytes. J Cardiovasc Electrophysiol 2000;11:665-676.
19. Meiry G, Reisner Y, Feld Y, Goldberg S, Rosen M, Ziv N, Binah O: Evolution of action potential propagation and repolarization in cultured neonatal rat ventricular myocytes. J Cardiovasc Electrophysiol 2001;12:1269-1277.
20. Zeng W, Morissette, Brochu R, Glass L, Shrier A: Complex rhythms resulting from overdrive suppression in electrically stimulated heart cell aggregates. Pacing Clin Electrophysiol 1990;13:1678-1685.
21. Amellal F, Hall K, Glass L, Billette J: Alternation of atrioventricular conduction time during atrioventricular reentrant tachycardia: Are dual pathways necessary? J Cardiovasc Electrophysiol 1996;7:943-951.
22. Sun J, Amellal F, Glass L, et al: Alternans and period doubling bifurcations in atriventricular nodal conduction. J Theor Biol 1995;173:79-91.
23. Simson MB, Spear JF, Moore EN: Stability of an experimental atrioventricular reentrant tachycardia in dogs. Am J Physiol 1981;240:H947-H953.
24. Cranefield PF: Action potentials after potentials, and arrhythmias. Circ Res 1977;41:415-423.
25. Volders PG, Vos MA, Szabo B, et al. Progress in the understanding of cardiac early afterdepolarizations and torsades de pointes: Time to revise current concepts. Cardiovasc Res 2000;46:376-392.
26. Bers DM: Control of cardiac contraction by SR Ca release and sarcolemmal Ca fluxes. In Bers DM, ed: *Excitation Contraction Coupling and Cardiac Contractile Force*. Dordrecht, The Netherlands: Kluwer, 1993, pp. 149-170.
27. January CT, Riddle JM: Early afterdepolarizations: Mechanism of induction and block. A role for L-type Ca^{2+} current. Circ Res 1989;64:977-990.
28. Roden DM: Early afterdepolarizations and torsade de pointes: Implications for the control f cardiac arrhythmias by prolonging repolarization. Eur Heart J 1993;14:51-61.
29. Viswanathan PC, Rudy Y: Pause induced early afterdepolarizations in long QT syndrome: A simulation study. Cardiovasc Res 1999;42:530-542.

30. Landau M, Lorente P, Henry J, Canu S: Hysteresis phenomena between periodic and stationary solutions in a model of pacemaker and nonpacemaker coupled cardiac cells. J Math Biol 1987;25:491-509.
31. Zimmerman M, Maisonblanche P, Cauchemez B, Leclercq JF, Coumel P: Determinants of the spontaneous ectopic activity in repetitive monomorphic idiopathic ventricular tachycardia. J Am Coll Cardiol 1986;7:1219-1227.
32. Lerman BB, Stein KS, Engelstein ED, Battlemen, DS, Lippman N, Bei D, Catanzaro D: Mechanism of repetitive monomorphic ventricular tachycardia. Circulation 1995;92:421-429.
33. Levine HD, Smith C: Repetitive paroxysmal tachycardia in adults: Prognosis–relationship to nervous system and to classical tachycardia. Cardiology 1970;55:2-21.
34. Lemery R, Brugada P, Bella PD, Dugernier T, Dool A, Wellens HJJ: Nonischemic ventricular tachycardia: Clinical course and long-term follow-up in patients without clinically overt heart disease. Circulation 1989;79:990-999.